



Published in final edited form as:

Anticancer Agents Med Chem. 2014 ; 14(7): 946–954.

Novel action and mechanism of auranofin in inhibition of vascular endothelial growth factor receptor-3-dependent lymphangiogenesis

Xiaodong Chen^{1,2}, Huanjiao Jenny Zhou^{1,2}, Qunhua Huang², Lin Lu^{1,4}, and Wang Min^{1,2,4}

¹State Key Laboratory of Ophthalmology, Zhongshan Ophthalmic Center, Sun Yat-sen University, Guangzhou, China

²Department of Pathology, Yale University School of Medicine

Abstract

Auranofin is a gold compound initially developed for the treatment of rheumatoid arthritis. Recent data suggest that auranofin has promise in the treatment of other inflammatory and proliferative diseases. However, the mechanisms of action of auranofin have not been well defined. In the present study, we identify vascular endothelial growth factor receptor-3 (VEGFR3), an endothelial cell (EC) surface receptor essential for angiogenesis and lymphangiogenesis, as a novel target of auranofin. In both primary EC and EC cell lines, auranofin induces downregulation of VEGFR3 in a dose-dependent manner. Auranofin at high doses ($\geq 1 \mu\text{M}$) decreases cellular survival protein thioredoxin reductase (TrxR2), TrxR2-dependent Trx2 and transcription factor NF- κ B whereas increases stress signaling p38MAPK, leading to EC apoptosis. However, auranofin at low doses ($\leq 0.5 \mu\text{M}$) specifically induces downregulation of VEGFR3 and VEGFR3-mediated EC proliferation and migration, two critical steps required for in vivo lymphangiogenesis. Mechanistically, we show that auranofin-induced VEGFR3 downregulation is blocked by antioxidant N-acetyl-L-cysteine (NAC) and lysosome inhibitor chloroquine, but was promoted by proteasomal inhibitor MG132. These results suggest that auranofin induces VEGFR3 degradation through a lysosome-dependent pathway. Auranofin may be a potent therapeutic agent for the treatment of lymphangiogenesis-dependent diseases such as lymphedema and cancer metastasis.

Keywords

Auranofin; lymphangiogenesis; thioredoxin reductase; vascular endothelial growth factor receptor-3

INTRODUCTION

The gold compound Auranofin is a metal phosphine complex that was developed for a treatment of rheumatoid arthritis as gold-based drugs¹. Recent data suggest that auranofin

⁴Corresponding author: Dr. Wang Min, Interdepartmental Program in Vascular Biology and Therapeutics, Department of Pathology, Yale University School of Medicine, 10 Amistad St., New Haven, CT 06520., Tel: 203-785-6047; Fax: 203-737-2293; wang.min@yale.edu or drlulin@126.com.

has promise in the treatment of other inflammatory and proliferative diseases². However, the mechanisms of action of auranofin have not been well defined.

Lymphatics play a substantial role in conditions such as chronic airway inflammation, tumor growth and metastasis, rheumatoid arthritis, inflammatory bowel disease, renal and corneal transplant rejection, and atopic dermatitis and psoriasis³. Lymphatic vessels express distinct cellular markers such as Prox-1, podoplanin⁴, lymphatic vessel endothelial hyaluronan receptor-1 (LYVE-1)⁵ as well as surface receptors VEGFR2 and VEGFR3. VEGFR3 is expressed in the blood endothelium during development, but is restricted to the lymphatics in the adult with the exception of few blood capillaries in some organs⁶ as well as the microvasculature of tumors and wounds⁷. Therefore, VEGFR3 is critical for lymphangiogenesis and lymphangiogenesis-associated diseases⁸.

To determine whether auranofin regulates lymphangiogenesis, we investigated the effects of auranofin on endothelial cell (EC) survival, proliferation and migration in the mouse lymphatic endothelial cell line (SVEC) and in primary human lymphatic EC (HLEC). Our data demonstrate that auranofin at high doses induces EC apoptosis while at low dose specifically inhibits VEGFR3 expression and VEGFR3-dependent EC proliferation and migration. To the best of our knowledge, this is the first report to demonstrate that auranofin inhibits VEGFR3 and lymphangiogenesis.

MATERIALS AND METHODS

Reagents

Auranofin, SB203580, NAC, and chloroquine were purchased from Sigma-Aldrich (St. Louis, MO). MG132 was from Millipore (Billerica, MA). VEGFR3 antibody for Western blotting was from eBioscience (San Diego, CA, USA) and for immunostaining was from R&D Systems (Minneapolis, MN). TrxR2 and Trx2 antibodies were from ABCAM (Cambridge, MA). Other primary antibodies were purchased from Cell Signaling Technology (Danvers, MA, USA). HRP-linked antibodies were from GE Healthcare Bio-Sciences Corp (Piscataway, NJ, USA). Alexa Fluor 488- or 594-conjugated secondary antibodies were from Life Technologies (Grand Island, NY, USA).

Cell culture

Human dermal lymphatic endothelial cells (HLEC) (HMVEC-dLyAd) were purchased from Lonza, and were cultured in EGM-1 MV media on cell culture dishes coated with fibronectin (10 µg/ml) as we described previously⁹. For characterization, cells were stained with Prox-1 and podoplanin, nuclear and transmembrane markers for HLEC, respectively. Earlier passage cells were >95% positive for LEC markers. All experiments were performed in early passages (passages 3–6) and cells remained Prox-1 positive. SVEC cell line (ATCC[®] CRL-2181[™]) is a mouse endothelial cell line derived by SV40 (strain 4A) transformation of endothelial cells from axillary lymph node vessels. SVEC cells were cultured in Dulbecco's modified Eagle's medium with 4mM L-glutamine adjusted to contain 1.5 g/L sodium bicarbonate and 4.5 g/L glucose, 10% heat-inactivated fetal bovine serum,

100 units/ml Penicillin, and 100 µg/ml Streptomycin, at 37°C in a humidified incubator with 5% CO₂ atmosphere.

Cell growth inhibition assay

[Berridge MV, Herst PM, and Tan AS. Tetrazolium dyes as tools in cell biology: new insights into their cellular reduction. *Biotechnology Annual Review*, 11: 127–152 (2005)]. The SVEC cells (1×10⁴/well) were seeded into 96-well culture plates and cultured at 37°C in a 5% CO₂/air environment for 12 h. After cells were treated with different dose of auranofin for 4–24 h, 10 µL solution of MTT (0.5mg/mL in PBS) was added to each well. After incubation 4h, the MTT agent was removed and the formazan particles were solubilized with 150 µl DMSO. The absorbance was read at 570 nm with a microplate reader X-wave BioTek Synergy (BioTek Instruments). Cell viability was expressed as a percentage of control.

Assay for Apoptosis

SVEC (10×10⁴/well) were seeded 12-well culture plates and cultured at 37°C in a humidified incubator with 5% CO₂ for 12 h. After cells were treated with 1 µM and 2 µM auranofin for 4h, Incubate the cells in 0.5mL Annexin-binding buffer 10 mM HEPES, 140 mM NaCl, and 2.5 mM CaCl₂, pH 7.4 with 5uL Annexin V conjugated Alexa-Fluor® 488 Life Technologies, A13201 and 1 uL Hoechst3342 (Life Technologies) at room temperature for 15 min. Apoptosis of cells were observed using a Zeiss Axiovert 200 fluorescence microscope (Carl ZeissMicroImaging; Thornwood, NY), and images were captured using Openlab3 software (Improvison, Lexington, MA).

Cell migration assay

For monolayer migration, SVEC were seeded in 12-well tissue culture plates and grown to confluence. Cells were serum starved for 12 h and were then subjected to “wound injury” assay with a 200 µl plastic pipette tip. Fresh media containing 3% serum alone or serum with VEGF-C (50 ng/m) in the absence or presence of 0.25 µM auranofin. Cell were cultured for 12 h. The SVEC migration in culture was determined by measuring wound areas in cell monolayers. Wound images were captured by a digital camera under a Zeiss Axiovert microscope (10X). Wound healing (% wound closure) was measured and analyzed by NIH Image 1.60⁹.

Gene expression

Total RNAs were isolated from cells by using the RNeasy kit with DNase I digestion (Qiagen, Valencia, CA). Reverse transcription (RT) was done by standard procedure (iScript™ cDNA Synthesis Kit) using 1µg total RNA. Quantitative real-time polymerase chain reaction (PCR) was performed by using iQ™ SYBR® Green Supermix on iCycler real time detection system iQ™ SYBR® Green Supermix (Bio-Rad Laboratories, Inc, Hercules, CA). RT-PCR with specific primers were described previously⁹.

BrdU incorporation assay in vitro

BrdU incorporation assay was performed as we described previously¹⁰. Briefly, SVEC were grown on 0.1% gelatin-coated glass chamber slides for 12 h. Cells were treated with 0.25 μ M auranofin for 12h, and then incubated with 10 μ M BrdU for 4 h prior to fixation with 4% PFA for 30 min at room temperature. Once fixed, cells were acid denatured with 2M HCl in 0.1% PBS-Tween for 30 min and then washed three times in PBS. Cells were then permeabilized and blocked nonspecific epitopes by 1%BSA/10% normal horse serum in 0.1% PBS-Tween for 1 h following by primary anti-BrdU antibody and secondary antibody incubation.

Western Blot Analysis

All Immunoblotting were performed as previously described¹⁰. In brief, SVEC were treated by auranofin, cells were washed two times by cold PBS and lysed in cold 1 \times SDS buffer. Then, protein samples were boiled for 10 min, resolved in 8~10% polyacrylamide gels and transferred to polyvinylidene difluoride membrane and blocked with 5% milk diluted in PBS containing 0.05 % Tween20 (PBST). Membranes were then immunoblotted with the specified antibodies (1:1000 dilution in PBST) using horseradish peroxidase-conjugated secondary antibodies (1:2,000 dilution; GE Healthcare Life Sciences/Amersham Biosciences) and enhanced chemiluminescence detection system (GE Healthcare Life Sciences, Amersham Biosciences).

Immunofluorescence microscopy (IF)

SVEC were grown on fibronectin-coated glass chamber slides for 12h. Cells were then treated by auranofin as indicated. Cells were fixed with 4% PFA in PBS for 15 min at room temperature, permeabilized with 0.1% triton-X buffer, blocked in 1% horse serum diluted in PBS for 1 h and stained 2 h at room temperature or 4 °C overnight using specified antibodies, followed by Alexa Fluor 488- or 594-conjugated secondary antibodies (donkey anti-goat, donkey anti-rabbit or donkey anti-mouse or a combination for double IF diluted at 1:1000 in PBST). Slides were observed using a Zeiss Axiovert 200 fluorescence microscope (Carl ZeissMicroImaging; Thornwood, NY), and images were captured using Openlab3 software (Improvision, Lexington, MA).

Statistical Analysis

Experiments were carried out at least in triplicate and results were expressed as mean \pm SEM. Statistical analysis was performed using SPSS statistical package (SPSS 16.0 for Windows; SPSS, Inc. Chicago, IL). Difference between two groups was analyzed by two-tailed Student's t test, and that between two or more groups was analyzed by one-way ANOVA multiple comparisons followed by Bonferroni's post-hoc test. Difference with P<0.05 (*) or P<0.01 (**) was considered statistically significant.

RESULTS

Auranofin inhibits cell growth and induces cell apoptosis in a dose-dependent manner

Studies in tumor cells have suggested that auranofin, a gold complex (Fig. 1A for structure), induces mitochondrial dysfunction and cell death^{1d, 11}. However, the responses of endothelial cells (EC) to auranofin have not been investigated. To this end, we examined the effects of auranofin on cell viability in primary EC and several EC lines by MTT assay. Auranofin treatment of SVEC (an SV40 T antigen-immortalized lymphatic EC line expressing both VEGFR2 and VEGFR3) resulted in decrease of EC viability in dose- and time-dependent manner. Treatment of auranofin for 12 h caused significant reduction of cell survival at $\geq 1 \mu\text{M}$ but not at lower doses (≤ 0.5) (Fig. 1B). Annexin-V and Hoechst-33342 double staining revealed that auranofin at $\geq 1 \mu\text{M}$ induced EC apoptosis (Fig. 1C with quantification in D). These data suggest that auranofin induces mitochondrial dysfunction and EC apoptosis at high concentrations.

Auranofin at a high dose inhibits EC survival and induces EC apoptosis

Auranofin has been shown as an inhibitor of thioredoxin reductase (TrxR; both cytosolic TrxR1 and mitochondrial TrxR2) and induces apoptosis in several cancer cell lines where auranofin at high doses activates ROS generation, p38 mitogen-activated protein kinase (p38MAPK) with reduction of the survival transcription factor NF- κ B^{1d, 11-12}. To elucidate the intracellular mechanisms of EC mitochondrial dysfunction and apoptosis induced by auranofin, we measured expression of TrxR2, Trx2, generation of ROS, activation of p38MAPK, and reduction NF- κ B activity. Correlating with the effects of auranofin on EC survival, auranofin at high doses ($\geq 1 \mu\text{M}$) induced significant reductions in expression of TrxR2 and Trx2 (Fig. 2A), the critical anti-oxidant system in the mitochondria¹³. Therefore, auranofin induced mitochondrial ROS generation in a concentration-dependent manner as measured by mitochondrial ROS probe Dihydrorhodamine 123, which can be blocked by anti-oxidant N-acetyl-cysteine (NAC) (Fig. 2B). Auranofin at high doses also induced phosphorylation of p38MAPK with a reduction in phosphorylations of NF- κ B as previously reported in other cell types. Interestingly, we observed significant reduction in expression of the EC-specific survival receptor VEGFR3 at various concentrations (Fig. 2A). As we reported recently⁹, protein analysis of VEGFR-3 by Western blot revealed 3 bands (Fig. 1E). While the band at 175 kDa is considered to be the intracellular and unglycosylated precursor, the band with molecular weight 125 kDa represents the mature form of VEGFR-3¹⁴. SVEC is immortalized EC cell line where another important survival receptor VEGFR2 is expressed at a very low level. We therefore examined effects of auranofin in primary human lymphatic EC (HLEC) which express both VEGFR3 and VEGFR2^{8a}. Auranofin induced activation of p38MAPK (Fig. 2C) and ROS generation (Fig. 2D) in HLEC as observed in SVEC. In these primary EC auranofin also induced a significant downregulation of VEGFR3 even at a low dose ($\leq 0.5 \mu\text{M}$), but only weakly reduced the expression of VEGFR2 (Fig. 2C).

Auranofin specifically reduces VEGFR3 at a low dose

We then investigate the mechanism by which auranofin at a low dose ($\leq 0.5 \mu\text{M}$) specifically downregulates VEGFR3 in SVEC. Cells were treated with a low dose of auranofin (0.25

μM) for various times (0–24 h), and VEGFR3 and protein were determined. Results indicated that auranofin induced downregulation of VEGFR3 protein without significant alterations on VEGFR3 mRNA (Fig. 3A). LYVE-1, a specific marker for lymphatic EC, was not affected by auranofin at its mRNA or its protein level. Auranofin at a low dose had no effect on the activation of p38MAPK (Fig. 3B). The downregulation of VEGFR3 in SVEC was further confirmed by indirect immunofluorescence staining. Consistent with the immunoblotting results, auranofin significantly reduced VEGFR3 immunostaining with no effects on LYVE-1 (Fig. 3C).

Auranofin induces VEGFR3 degradation via a lysosome-dependent pathway

Recently we have demonstrated that VEGFR3 stability is regulated in EC¹⁰. Since VEGFR3 mRNA was not significantly altered by auranofin, we examined how VEGFR3 protein is regulated by auranofin. We first examined if auranofin induced ROS generation is required for VEGFR3 downregulation. SVEC were incubated with auranofin in the absence or presence of anti-oxidant NAC or p38MAPK inhibitor SB203580 compound. Consistent with that auranofin at 0.25 μM induces a low level of ROS but not activation of p38MAPK, auranofin-induced VEGFR3 downregulation was blocked by NAC but not by p38MAPK inhibitor (Fig. 4A). Of note, p38MAPK inhibitor (which blocks p38MAPK kinase activity towards its substrates) stabilized phosphor-p38MAPK.

To determine which degradation pathway is involved in VEGFR3 degradation, SVEC were treated with auranofin in the presence of proteasomal inhibitor MG132 or lysosomal inhibitor chloroquine (CHQ)¹⁵. Results showed that CHQ, but not MG132, significantly blocked auranofin-induced VEGFR3 degradation in SVEC (Fig. 4B). Surprisingly, MG132 alone strongly induced degradation of VEGFR3. These data indicate that auranofin induces VEGFR3 downregulation through a lysosome-dependent degradation pathway.

Auranofin at a low dose inhibits VEGFR3-dependent EC proliferation and migration

We have recently shown that VEGFR3 is critical for VEGF-C-induced EC proliferation and migration, two critical steps for lymphangiogenesis in vivo^{9–10}. We finally examined the effects of auranofin on VEGF-C-induced SVEC proliferation and migration. The effect of auranofin on SVEC proliferation was detected by BrdU incorporation assay in vitro. Under normal culture media with growth factors containing VEGF-C, treatment of auranofin at 0.25 μM for 12h significantly reduced BrdU⁺ SVEC cells (Fig. 5A with quantification in 5B), suggesting that a low dose of auranofin reduced SVEC proliferation.

To determine effects of auranofin on EC migration, SVEC migration was stimulated with VEGF-C in the presence or absence of 0.25 μM of auranofin, and cell migration was assessed by a scratch wound assay. Auranofin significantly reduced both basal and VEGF-C-induced wound closure with more profound effects on VEGF-C-induced EC migration (Fig. 5C with quantifications in 5D by comparing ARF effects on basal and VEGF-C-induced migration). In other words, VEGF-C had stronger responses in promoting LEC migration in the absence of auranofin (Fig. 5E by comparing VEGF-C responses in the absence and presence of ARF). In contrast, High doses ($\geq 1 \mu\text{M}$) of auranofin induced LEC apoptosis and completely blocked both basal and VEGF-C-induced LEC migration (not shown). These

data indicate that auranofin at a low dose specifically inhibits VEGFR3-dependent lymphangiogenesis.

DISCUSSION

In the present study, the molecular mechanisms underlying the auranofin-induced inhibition of lymphangiogenesis *in vitro* were investigated. The results of this study are summarized in a schematic representation (Fig. 6). Auranofin at a high dose causes cell apoptosis by downregulating survival factors TrxR2, Trx2 and NF- κ B, while activating p38MAPK, leading to EC apoptosis (see Fig. 1) and complete blockade of EC migration. Auranofin at a low dose inhibits VEGFR3 expression, VEGFR3-dependent EC proliferation and migration. Therefore, we have identified VEGFR3 as a novel target of auranofin. Moreover, we show that auranofin-induced VEGFR3 downregulation is blocked by antioxidant NAC and lysosome inhibitor chloroquine, but promoted by proteasomal inhibitor MG132. Our data reveal a novel mechanism by which auranofin specifically regulates VEGFR3 degradation through a lysosome-dependent pathway in lymphatic EC.

Auranofin has been widely used as a Trx reductase inhibitor. Therefore, despite the decline in its clinical applications in rheumatoid arthritis, auranofin shows promise in the treatment of several different diseases, including leukemia, carcinoma, and parasite, bacterial and viral infections. This is because the Trx reductase system and its thiol redox activity are important for cell survival and proliferation^{13a, 16}. TrxR2 converts Trx2 from an oxidized inactive form of Trx2 to a reduced active. Our results show that auranofin treatment causes reduction of Trx2 protein, suggesting that TrxR2 may stabilize Trx2 in EC and oxidized Trx2 is more accessible for degradation. Auranofin induces ROS generation and ROS-activated p38MAPK in EC, likely resulting from the reduction of the TrxR2-Trx2 proteins¹³. In addition, Trx reductase is also known to maintain NF- κ B p65 protein stability^{1d, 11-12, 16-17}. Consistent with this notion, we have observed that auranofin, by inhibiting Trx reductase activity, induces downregulation of NF- κ B p65.

Auranofin, as Trx reductase inhibitor, has also been used as a tool to define cellular thiol-dependent signaling pathway and their functions. For example, Auranofin was used by Dr. Dean Jones group to specifically inhibit Trx reductase without oxidation of the GSH/GSSG while buthionine sulfoximine was used to deplete GSH without detectable oxidation of Trx1. Based on this specificity of auranofin, they have shown that auranofin can modify proteins associated with cellular glycolysis, cytoskeleton remodeling, protein translation and cell adhesion¹⁸. Consistent with their findings, we have observed that auranofin at a high dose (2 μ M) strongly disrupts cytoskeleton and EC-junctions as visualized by phalloidin and anti-ZO-1, respectively (Supplemental Fig. S1).

The most novel finding in our work, by examining effects of auranofin at a low dose on lymphatic EC, is the identification of VEGFR3 as a specific target of auranofin. Auranofin at a low dose does not induce EC apoptosis, correlating with its lack of effect on protein expression of TrxR2, Trx2, NF- κ B p65 or p38MAPK activation. However, auranofin at a low dose specifically reduces VEGFR3 protein in both immortalized lymphatic EC lines and primary lymphatic EC with no effect on lymphatic EC marker LYVE-1. Since auranofin at a low

dose reduces VEGFR3 protein but not VEGFR3 mRNA levels, we have explored potential mechanisms by which auranofin induces VEGFR3 degradation. Our surprising finding is that a lysosomal inhibitor chloroquine, but not a proteasomal inhibitor MG132, blocks auranofin-induced VEGFR3 degradation; MG132 in fact induced VEGFR3 degradation. Our results clearly support that auranofin induces VEGFR3 downregulation through a lysosome-dependent degradation pathway. The exact mechanism by which auranofin induces a lysosome-dependent degradation is unclear. Recent studies have suggested that VEGFR3 surface and protein stability are regulated by endocytosis, mediated by AIP1, Dab2, the transmembrane protein Ephrin B2 and the cell polarity regulator Par-3^{10, 19}. It is plausible that auranofin induces endocytosis of VEGFR3 in lymphatic EC by modulating the AIP1-Dab2-Ephrin-Par3 complex. Meanwhile, auranofin may also prevent VEGFR-3 recycling or/and promote VEGFR-3 trafficking to lysosome. We are currently investigating this possibility. Consistent with that auranofin at a low dose induces a low level of ROS but not activation of p38MAPK, auranofin-induced VEGFR3 downregulation was blocked by NAC but not by p38MAPK inhibitor SB203580. The role of ROS in promoting VEGFR3 endocytosis needs to be further determined.

The generation of new lymphatic vessels through lymphangiogenesis and the remodelling of existing lymphatics are thought to be important steps in cancer metastasis^{8b}. The VEGF-C/VEGFR3 axis is considered to be a major driver of tumour lymphangiogenesis⁶⁻⁷. Our study demonstrate that auranofin specifically inhibits the VEGF-C/VEGFR3-dependent lymphangiogenesis. Our study suggests auranofin as therapeutic agent for the treatment of lymphangiogenesis-mediated disease such as such as lymphedema and cancer metastasis⁸.

Supplementary Material

Refer to Web version on PubMed Central for supplementary material.

Acknowledgments

This work was supported by the National Institutes of Health grants HL109420 and HL115148 to W. Min; and the grant No.81170863 from National Nature Science Foundation of China to L. Lu. XC is Sun Yat-sen University-sponsored scholar; JZ is a Chinese Scholar Council (CSC)-sponsored scholar.

References

1. (a) Finkelstein AE, Walz DT, Batista V, Mizraji M, Roisman F, Misher A. Auranofin. New oral gold compound for treatment of rheumatoid arthritis. *Ann Rheum Dis.* 1976; 35(3):251–7. [PubMed: 791161] (b) Glennas A, Kvien TK, Andrup O, Clarke-Jenssen O, Karstensen B, Brodin U. Auranofin is safe and superior to placebo in elderly-onset rheumatoid arthritis. *British journal of rheumatology.* 1997; 36(8):870–7. [PubMed: 9291856] (c) Gabbiani C, Messori L. Protein targets for anticancer gold compounds: mechanistic inferences. *Anti-cancer agents in medicinal chemistry.* 2011; 11(10):929–39. [PubMed: 21864237] (d) Casini A, Messori L. Molecular mechanisms and proposed targets for selected anticancer gold compounds. *Current topics in medicinal chemistry.* 2011; 11(21):2647–60. [PubMed: 22039866]
2. (a) Matsubara T, Ziff M. Inhibition of human endothelial cell proliferation by gold compounds. *J Clin Invest.* 1987; 79(5):1440–6. [PubMed: 3106416] (b) Madeira JM, Gibson DL, Kean WF, Klegeris A. The biological activity of auranofin: implications for novel treatment of diseases. *Inflammopharmacology.* 2012; 20(6):297–306. [PubMed: 22965242]

3. (a) Baluk P, Yao LC, Feng J, Romano T, Jung SS, Schreiter JL, Yan L, Shealy DJ, McDonald DM. TNF-alpha drives remodeling of blood vessels and lymphatics in sustained airway inflammation in mice. *J Clin Invest*. 2009; 119(10):2954–64. [PubMed: 19759514] (b) Stacker SA, Caesar C, Baldwin ME, Thornton GE, Williams RA, Prevo R, Jackson DG, Nishikawa S, Kubo H, Achen MG. VEGF-D promotes the metastatic spread of tumor cells via the lymphatics. *Nat Med*. 2001; 7(2):186–91. [PubMed: 11175849] (c) Mandriota SJ, Jussila L, Jeltsch M, Compagni A, Baetens D, Prevo R, Banerji S, Huarte J, Montesano R, Jackson DG, Orci L, Alitalo K, Christofori G, Pepper MS. Vascular endothelial growth factor-C-mediated lymphangiogenesis promotes tumour metastasis. *Embo J*. 2001; 20(4):672–82. [PubMed: 11179212] (d) Vass DG, Hughes J, Marson LP. Restorative and rejection-associated lymphangiogenesis after renal transplantation: friend or foe? *Transplantation*. 2009; 88(11):1237–9. [PubMed: 19996921] (e) Bruyere F, Noel A. Lymphangiogenesis: in vitro and in vivo models. *FASEB J*. 2010; 24(1):8–21. [PubMed: 19726757] (f) Halin C, Detmar M. Chapter 1. Inflammation, angiogenesis, and lymphangiogenesis. *Methods Enzymol*. 2008; 445:1–25. [PubMed: 19022053]
4. Breiteneder-Geleff S, Soleiman A, Horvat R, Amann G, Kowalski H, Kerjaschki D. Podoplanin--a specific marker for lymphatic endothelium expressed in angiosarcoma. *Verh Dtsch Ges Pathol*. 1999; 83:270–5. [PubMed: 10714221]
5. Banerji S, Ni J, Wang SX, Clasper S, Su J, Tammi R, Jones M, Jackson DG. LYVE-1, a new homologue of the CD44 glycoprotein, is a lymph-specific receptor for hyaluronan. *J Cell Biol*. 1999; 144(4):789–801. [PubMed: 10037799]
6. (a) Karpanen T, Alitalo K. Molecular biology and pathology of lymphangiogenesis. *Annu Rev Pathol*. 2008; 3:367–97. [PubMed: 18039141] (b) Tammela T, Alitalo K. Lymphangiogenesis: Molecular mechanisms and future promise. *Cell*. 2010; 140(4):460–76. [PubMed: 20178740] (c) Kaipainen A, Korhonen J, Mustonen T, van Hinsbergh VW, Fang GH, Dumont D, Breitman M, Alitalo K. Expression of the *fms*-like tyrosine kinase 4 gene becomes restricted to lymphatic endothelium during development. *Proc Natl Acad Sci U S A*. 1995; 92(8):3566–70. [PubMed: 7724599]
7. (a) Valtola R, Salven P, Heikkila P, Taipale J, Joensuu H, Rehn M, Pihlajaniemi T, Weich H, deWaal R, Alitalo K. VEGFR-3 and its ligand VEGF-C are associated with angiogenesis in breast cancer. *Am J Pathol*. 1999; 154(5):1381–90. [PubMed: 10329591] (b) Paavonen K, Puolakkainen P, Jussila L, Jahkola T, Alitalo K. Vascular endothelial growth factor receptor-3 in lymphangiogenesis in wound healing. *Am J Pathol*. 2000; 156(5):1499–504. [PubMed: 10793061]
8. (a) Jones D, Min W. An overview of lymphatic vessels and their emerging role in cardiovascular disease. *J Cardiovasc Dis Res*. 2011; 2(3):141–52. [PubMed: 22022141] (b) Stacker SA, Williams SP, Karnezis T, Shayan R, Fox SB, Achen MG. Lymphangiogenesis and lymphatic vessel remodelling in cancer. *Nat Rev Cancer*. 2014; 14(3):159–72. [PubMed: 24561443]
9. (a) Jones D, Li Y, He Y, Xu Z, Chen H, Min W. Mirtron MicroRNA-1236 Inhibits VEGFR-3 Signaling During Inflammatory Lymphangiogenesis. *Arterioscler Thromb Vasc Biol*. 2012; 32(3):633–42. [PubMed: 22223733] (b) Jones D, Xu Z, Zhang H, He Y, Kluger MS, Chen H, Min W. Functional Analyses of the Nonreceptor Kinase Bone Marrow Kinase on the X Chromosome in Vascular Endothelial Growth Factor-Induced Lymphangiogenesis. *Arterioscler Thromb Vasc Biol*. 2010; 30(12):2553–61. [PubMed: 20864667]
10. Zhou HJ, Chen X, Huang Q, Liu R, Zhang H, Wang Y, Jin Y, Liang X, Lu L, Xu Z, Min W. AIP1 Mediates Vascular Endothelial Cell Growth Factor Receptor-3-Dependent Angiogenic and Lymphangiogenic Responses. *Arterioscler Thromb Vasc Biol*. 2014; 34(3):603–15. [PubMed: 24407031]
11. Zhang H, Du Y, Zhang X, Lu J, Holmgren A. Glutaredoxin 2 Reduces Both Thioredoxin 2 and Thioredoxin 1 and Protects Cells from Apoptosis Induced by Auranofin and 4-Hydroxynonenal. *Antioxid Redox Signal*. 2014
12. (a) Park SJ, Kim IS. The role of p38 MAPK activation in auranofin-induced apoptosis of human promyelocytic leukaemia HL-60 cells. *Br J Pharmacol*. 2005; 146(4):506–13. [PubMed: 16086031] (b) Nakaya A, Sagawa M, Muto A, Uchida H, Ikeda Y, Kizaki M. The gold compound auranofin induces apoptosis of human multiple myeloma cells through both down-regulation of STAT3 and inhibition of NF-kappaB activity. *Leukemia research*. 2011; 35(2):243–9. [PubMed: 20542334]

13. (a) Powis G, Montfort WR. Properties and biological activities of thioredoxins. *Annu Rev Pharmacol Toxicol.* 2001; 41:261–95. [PubMed: 11264458] (b) Lee S, Kim SM, Lee RT. Thioredoxin and Thioredoxin Target Proteins: From Molecular Mechanisms to Functional Significance. *Antioxid Redox Signal.* 2013; 18(10):1165–207. [PubMed: 22607099] (c) Lu J, Holmgren A. Thioredoxin system in cell death progression. *Antioxid Redox Signal.* 2012; 17(12):1738–47. [PubMed: 22530689]
14. (a) Pajusola K, Aprelikova O, Pelicci G, Weich H, Claesson-Welsh L, Alitalo K. Signalling properties of FLT4, a proteolytically processed receptor tyrosine kinase related to two VEGF receptors. *Oncogene.* 1994; 9(12):3545–55. [PubMed: 7970715] (b) Bando H, Brokelmann M, Toi M, Alitalo K, Sleeman JP, Sipos B, Grone HJ, Weich HA. Immunodetection and quantification of vascular endothelial growth factor receptor-3 in human malignant tumor tissues. *Int J Cancer.* 2004; 111(2):184–91. [PubMed: 15197769]
15. Li M, Khambu B, Zhang H, Kang JH, Chen X, Chen D, Vollmer L, Liu PQ, Vogt A, Yin XM. Suppression of lysosome function induces autophagy via a feedback down-regulation of MTOR complex 1 (MTORC1) activity. *J Biol Chem.* 2013; 288(50):35769–80. [PubMed: 24174532]
16. Arner ES, Holmgren A. Physiological functions of thioredoxin and thioredoxin reductase. *Eur J Biochem.* 2000; 267(20):6102–9. [PubMed: 11012661]
17. Sakurai A, Yuasa K, Shoji Y, Himeno S, Tsujimoto M, Kunimoto M, Imura N, Hara S. Overexpression of thioredoxin reductase 1 regulates NF-kappa B activation. *J Cell Physiol.* 2004; 198(1):22–30. [PubMed: 14584040]
18. Go YM, Roede JR, Walker DI, Duong DM, Seyfried NT, Orr M, Liang Y, Pennell KD, Jones DP. Selective targeting of the cysteine proteome by thioredoxin and glutathione redox systems. *Mol Cell Proteomics.* 2013; 12(11):3285–96. [PubMed: 23946468]
19. (a) Nakayama M, Berger P. Coordination of VEGF receptor trafficking and signaling by coreceptors. *Exp Cell Res.* 2013; 319(9):1340–7. [PubMed: 23499743] (b) Benedito R, Rocha SF, Woeste M, Zamykal M, Radtke F, Casanovas O, Duarte A, Pytowski B, Adams RH. Notch-dependent VEGFR3 upregulation allows angiogenesis without VEGF-VEGFR2 signalling. *Nature.* 2012; 484(7392):110–4. [PubMed: 22426001] (c) Nakayama M, Nakayama A, van Lessen M, Yamamoto H, Hoffmann S, Drexler HC, Itoh N, Hirose T, Breier G, Vestweber D, Cooper JA, Ohno S, Kaibuchi K, Adams RH. Spatial regulation of VEGF receptor endocytosis in angiogenesis. *Nat Cell Biol.* 2013; 15(3):249–60. [PubMed: 23354168]

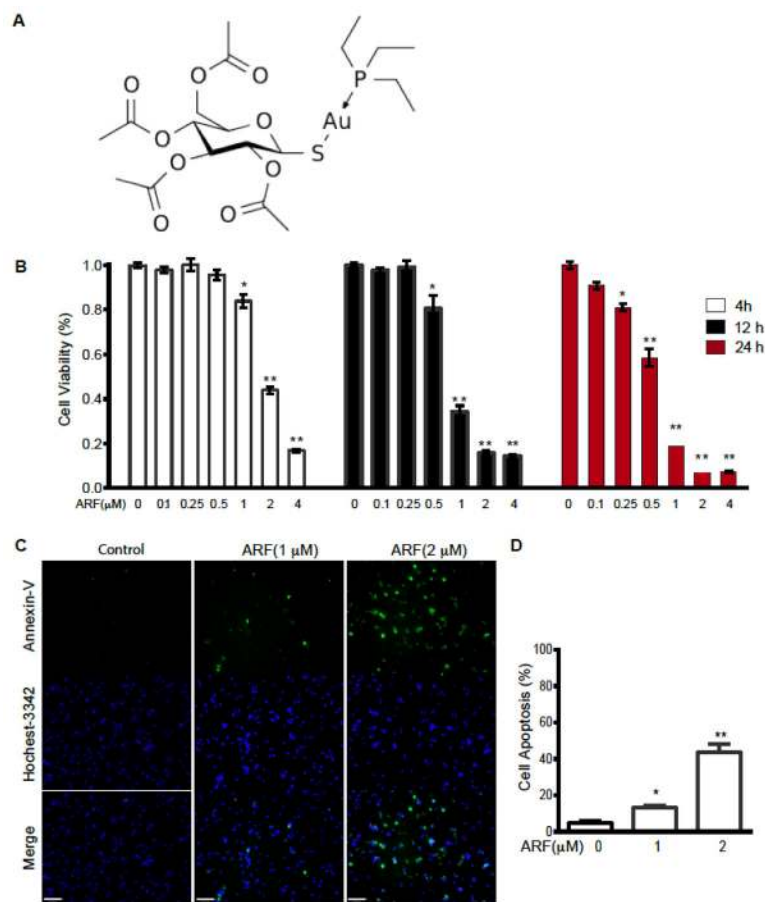


Fig. 1. Auranofin inhibits EC survival and induces cell apoptosis in a dose-dependent manner

A. Auranofin structure: gold(+1) cation; 3,4,5-triacetyloxy-6- (acetyloxymethyl) oxane-2-thiolate; triethylphosphonium (formula $C_{20}H_{35}AuO_9PS^+$). **B.** SVEC were treated with ARF at 0–4 μM for indicated times (4, 12 and 24 h). EC viability was measured by a mitochondrial activity-based MTT assay and % of control were presented. Data are mean \pm SEM from triplicates of three independent experiments. *, $P < 0.05$; **, $P < 0.01$. **C.** SVEC were treated with ARF at 0, 1 or 2 μM for 4 h. EC apoptosis was measured by Annexin-V and Hoechst-3342 double staining. Scale bar: 100 μm . **D.** EC apoptosis (%) was quantitated. Data are mean \pm SEM from duplicates (10 different areas in each well) of three independent experiments. *, $P < 0.05$; **, $P < 0.01$.

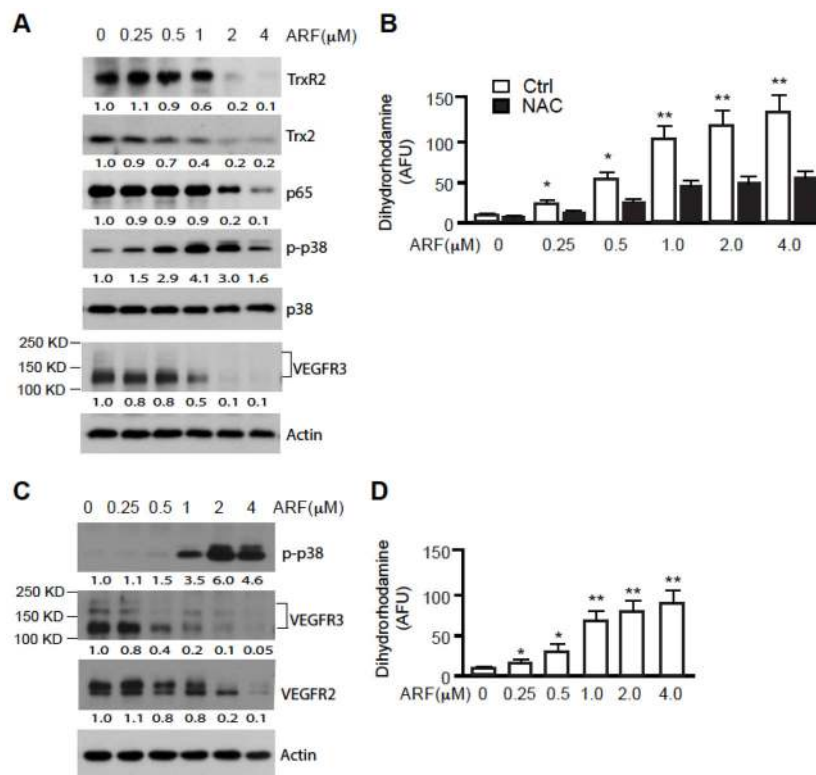


Fig. 2. Auranofin at a high dose inhibits EC survival while inducing apoptotic pathways SVEC (A, B) or HLEC (C, D) were treated with ARF at 0–4 μM for 4 h. **A** and **C**. Cell lysates were subjected to immunoblotting for TrxR2, Trx2, NF-κB, phosphor- and total p38MAPK, and VEGFR3 with respective antibodies. β-actin was used as a loading control. Normalized protein levels are indicated below the blot with untreated as 1.0. Relative ratios of p-p38MAPK and total p38MAPK are also indicated. Similar results were obtained from additional two experiments. **B** and **D**. ROS levels from ARF-treated SVEC were measured by Dihydrorhodamine 123 probe in a fluorescence plate reader for 120 min. Data presented are mean±SEM from triplicates of three independent experiments. *, $P < 0.05$; **, $P < 0.01$.

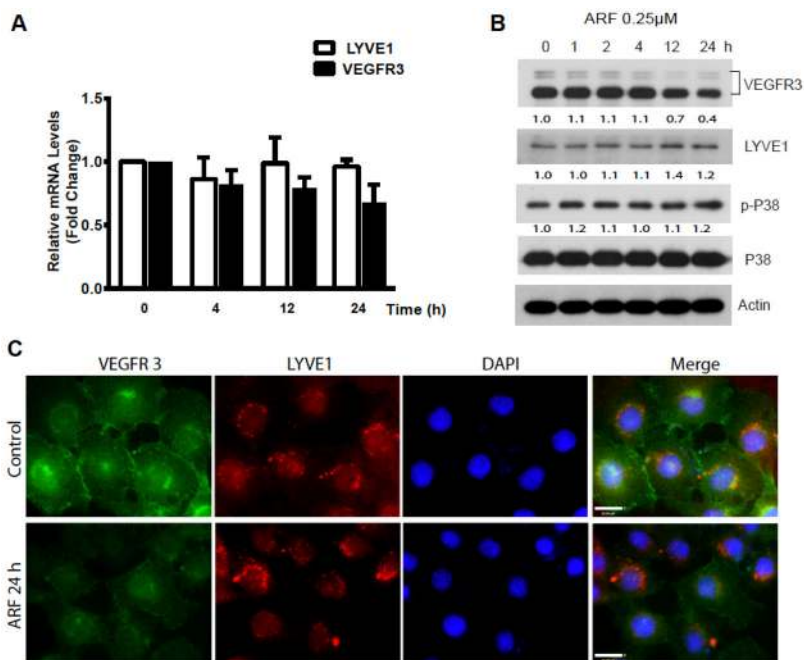


Fig. 3. Auranofin specifically reduces VEGFR3 at a low dose

SVEC were treated with ARF (0.25 μ M) for various times (0–24 h). **A.** VEGFR3 and LYVE-1 mRNA were quantified by qRT-PCR with respective primers. Relative levels of VEGFR3 and LYVE-1 mRNA are presented as untreated cells as 1.0. Data presented are mean \pm SEM from three independent experiments. **B.** Cell lysates were subjected to immunoblotting for phosphor- and total p38MAPK, VEGFR3 and lymphatic EC surface marker LYVE-1 with respective antibodies. β -actin was used as a loading control. Normalized protein levels of VEGFR3 and LYVE-1 as well as ratios of p-p38/p38 are indicated below the blot with untreated as 1.0. LYVE-1 is a surface marker for lymphatic EC, and ARF had no effects on LYVE-1 protein levels. **C.** ARF-induced VEGFR3 downregulation in SVEC was measured by immunofluorescence staining. SVEC were treated with ARF (0.25 μ M) for 24 h. VEGFR3 and LYVE-1 were detected by immunostaining with respective antibodies followed by Alexa Fluor 488 and 594-conjugated secondary antibodies.

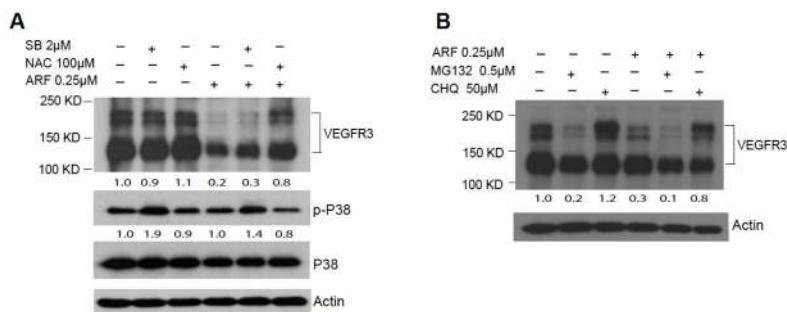


Fig. 4. Auranofin induces VEGFR3 degradation via a lysosome-dependent pathway

A. SVEC were incubated with ARF (0.25 μ M) in the presence of anti-oxidant NAC (100 μ M) or p38MAPK (2 μ M) for 24 h. Cell lysates were subjected to immunoblotting for phosphor-, total p38MAPK and VEGFR3 with respective antibodies. β -actin was used as a loading control. Normalized VEGFR3 protein levels and ratios of p-p38/p38 are indicated below the blot with untreated as 1.0. Similar results were obtained from additional two experiments. **B.** SVEC cells were incubated with ARF (0.25 μ M) in the presence of MG132 (0.5 μ M) or chloroquine (50 μ M) for 12 h. Cell lysates were subjected to immunoblotting for VEGFR3 and β -actin with respective antibodies. Normalized VEGFR3 protein levels are indicated below the blot with untreated as 1.0. Similar results were obtained from additional two experiments.

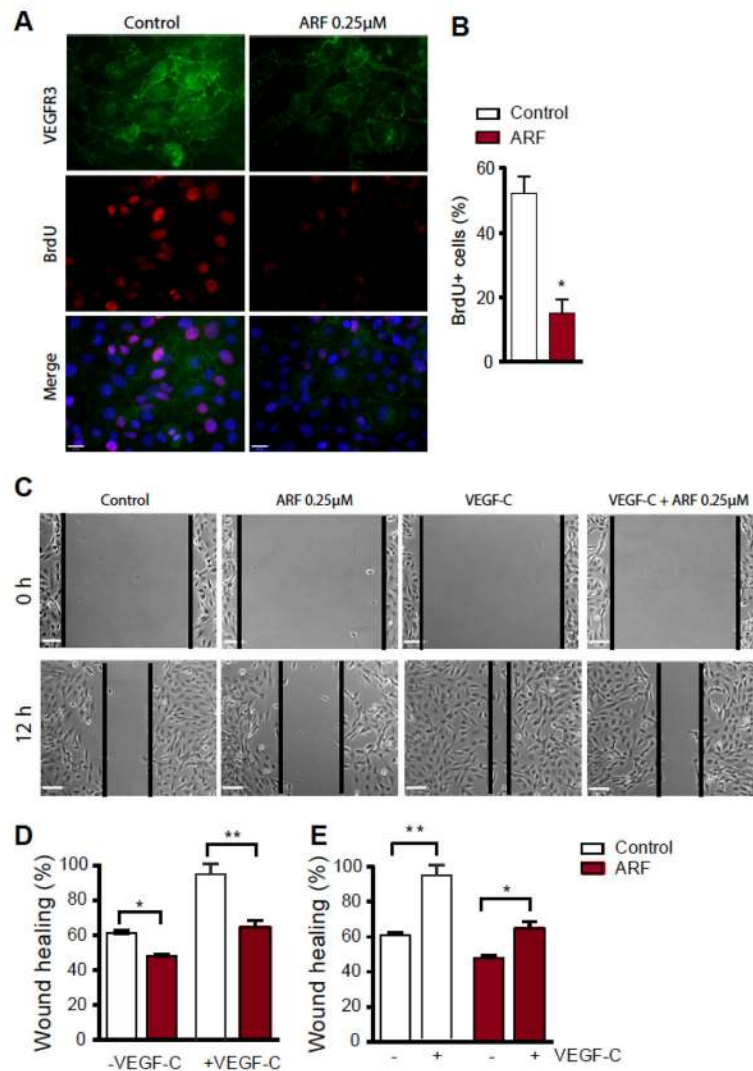


Fig. 5. Auranofin at a low dose inhibits VEGFR3-dependent EC proliferation and migration
A–B. SVEC were treated with ARF at 0.25 µM for 12h, and cells were subjected to BrdU labeling for 4 h followed by immunostaining with anti-VEGFR3 and anti-BrdU. Representative images are shown in **A** and BrdU+ cells were quantified in **B**. Data are mean ±SEM from duplicates (5 different areas in slide) of three independent experiments. *, $P < 0.05$. **C–D.** SVEC were cultured 3% serum without growth factors and subjected to “wound” injury assay. Cells were untreated or stimulated with VEGF-C (50 ng/ml) in the absence or presence of ARF (0.25 µM) for 12 h. Representative images are shown in **C**. Scale bar, 100 µm. Cell migration distances were measured and % wound closure was quantified in **D** and **E**. Data are mean ±SEM from duplicates (10 different areas in each well) of three independent experiments. *, $P < 0.05$.

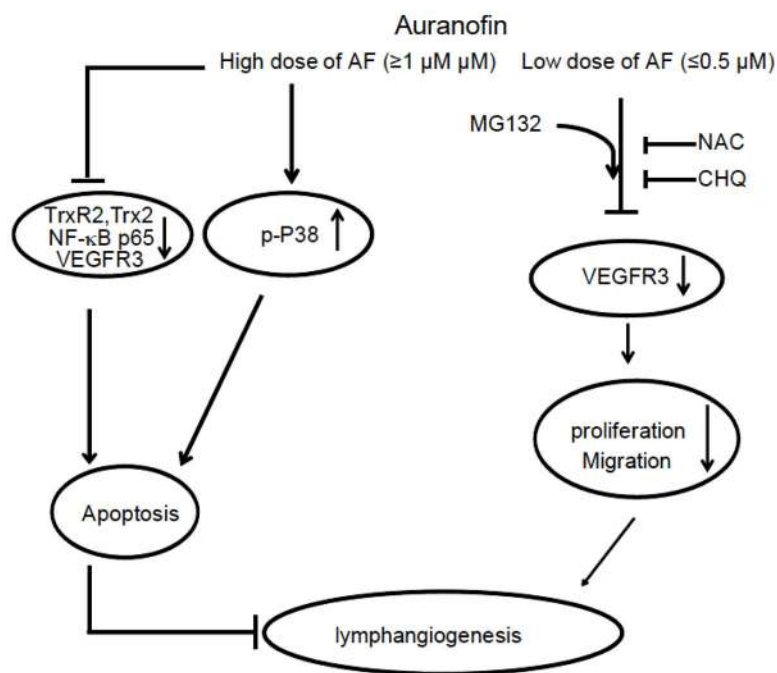


Fig. 6. A proposed model for auranofin inhibitory effects on lymphangiogenesis

Auranofin at a high dose causes cell apoptosis by downregulating survival factors TrxR2, Trx2 and NF- κ B, while activating p38MAPK, leading to EC apoptosis. Auranofin at a low dose inhibits VEGFR3 expression, VEGFR3-dependent EC proliferation and migration (see text for more details).